*J. exp. Biol.* **125**, 137–155 (1986)
*Printed in Great Britain* © *The Company of Biologists Limited 1986*



# PULMONARY MECHANICS AND THE WORK OF BREATHING IN THE SEMI-AQUATIC TURTLE, *PSEUDEMYS SCRIPTA*

BY TIMOTHY Z. VITALIS* AND WILLIAM K. MILSOM

*Department of Zoology, University of British Columbia, Vancouver, British Columbia, V6T 2A9 Canada*

*Accepted 18 April 1986*

## SUMMARY

Measurements of pulmonary mechanics on anaesthetized specimens of the aquatic turtle *Pseudemys scripta* (Schoepff) indicate that the static pulmonary mechanics of the total respiratory system are determined primarily by the mechanics of the body wall rather than those of the lungs. This is also true under the dynamic conditions of pump ventilation at low pump frequencies. As pump frequency increases, the work required to inflate the multicameral lungs of the turtle begins to contribute an increasing portion to the total mechanical work required to produce each breath as measured from pressure volume loops. The rise in the work performed on the lungs results from an increase in the non-elastic, flow-resistive forces which must be overcome during ventilation. The primary bronchus to each lung is the most likely site of flow resistance. There is also a small elastic component to the work required to ventilate the lungs associated with movement of the intrapulmonary septa and the striated muscle surrounding the lungs. The contribution of the work required to distend the body cavity as a percentage of the total mechanical work required to generate each breath remains relatively unchanged with increasing ventilation frequency, indicating that the majority of the forces to be overcome in the body wall are elastic in nature. For a constant rate of minute pump ventilation, as frequency increases, the work done per minute to overcome elastic forces decreases, while that done to overcome non-elastic forces begins to rise. These opposing trends produce an optimum combination of pump volume and frequency at which the rate of mechanical work is minimum.

## INTRODUCTION

It has been shown in mammals that for any given level of alveolar ventilation ($\dot{V}_A$) there is a combination of tidal volume ($V_T$) and breathing frequency (f) which minimizes the mechanical power required for ventilation (Otis, Fenn & Rahn, 1950). More power is required to ventilate the lungs if breathing frequency is above or below this 'optimal' rate for a constant level of ventilation. The spontaneous

* Present address: School of Biological Sciences, University of East Anglia, Norwich, NR4 7TJ, UK.

Key words: reptiles, pulmonary mechanics, work of breathing.

breathing pattern of many mammals corresponds very closely with their predicted optimal pattern (Christie, 1953; Agostoni, Thimm & Fenn, 1959; Crosfill & Widdicombe, 1961; Yamashiro, Daubenspeck, Lauritsen & Grodins, 1975).

In reptiles, normal breathing at rest is intermittent, unlike mammals where breathing is continuous. The reptilian pattern is characterized by single breaths or bursts of breaths separated by breath-holds of varying duration (McCutcheon, 1943; Gans & Hughes, 1967; Naifeh *et al.* 1970; Gans & Clark, 1976; Glass & Johansen, 1976). The primary variable that changes if breathing is stimulated by hypoxia, hypercapnia or increased temperature is the breath-hold period (Glass & Johansen, 1976; Milsom & Jones, 1980; Benchetrit & Dejours, 1980), while the response to exercise in lizards is characterized by increases in tidal volume (Wood & Lenfant, 1976; Cragg, 1978). Very little is known about the relationship between the work of breathing and the breathing patterns or respiratory response of intermittent breathers.

The static compliances of the lung and total respiratory system have been measured in a few reptile species, and Perry & Duncker (1978, 1980) have attempted to correlate resting breathing patterns with these static compliances. Such analysis, however, is limited since respiration is an active rather than a static process. An understanding of dynamic as well as static pulmonary mechanics is essential for assessing the mechanical factors influencing breathing patterns.

Only one such study has been performed on a non-homeothermic species. Milsom & Vitalis (1984) have shown that, in the Tokay gecko, both the dynamic and static mechanics are most strongly influenced by the mechanics of the body cavity and chest wall. The unicameral lungs of this species are relatively large and compliant and offer little resistance to air flow. Most of the work required to ventilate the lungs is used to overcome elastic forces in the chest wall alone, regardless of ventilation frequency. Similar values are reported in the literature for the body wall compliance of lizards and mammals of similar size. The highly developed, alveolar lungs of mammals, however, are very stiff by comparison with reptile lungs (Crosfill & Widdicombe, 1961; Perry & Duncker, 1978; Milsom & Vitalis, 1984) so that pulmonary mechanics in mammals are more strongly influenced by the properties of the lungs. In mammals, work is required to overcome both elastic and non-elastic forces during breathing (Agostoni, 1970; Crosfill & Widdicombe, 1961; Otis *et al.* 1950). Despite these differences, there is still a combination of tidal volume and frequency in the gecko which gives minimum values for the mechanical power required for each level of alveolar ventilation.

The aim of the following experiments is to extend such studies of static and dynamic pulmonary mechanics to the turtle, *Pseudemys scripta*. The multicameral lungs of the turtle are less complex than mammalian lungs but more complex than those of lizards. The bony carapace of the turtle should make the body wall very stiff. Given this unique combination of features, it is of interest to see how the differences in the architecture of the lungs and body wall are reflected in the mechanics of the respiratory system and to what extent dynamic mechanics can be used in predicting likely patterns of ventilation in intermittent breathers.

## MATERIALS AND METHODS

### *Static pressure–volume relationships*

The static pressure–volume relationships of the respiratory system were measured on eight turtles (726·3 ± 107 g body weight) maintained at room temperature (20–22 °C) and anaesthetized with 20–30 mg $kg^{-1}$ sodium pentobarbital (Somnotol, MTC Pharmaceuticals). In all animals, once signs of reflex activity were absent, the cloaca was sutured shut to prevent water loss from the urinary bladder which would have altered body volume and thus the mechanics of the body cavity and body wall. The trachea was cannulated *via* a midline incision just below the larynx which was then sewn closed. The cannula consisted of a short piece of PE 220 tubing with a side-arm for pressure measurements. Starting with the animals in a supine position and the tracheal cannula open to the atmosphere, the lungs were first inflated, then deflated and reinflated to a volume of 11 ml 100 $g^{-1}$ body weight with an air-filled syringe. This volume corresponds to the resting lung volume (VLR), as determined for this species by Jackson (1971), and the pressures associated with VLR in both the body compartment and lungs under these conditions are referred to as zero pressure for these static pressure–volume relationships. We were confident that this technique of deflating the lungs with a syringe removed all gas from the animal's lungs. Unlike the mammalian alveolar lung with its highly branched bronchial tree, the multicameral lungs of the turtle collapse completely when deflated. Any residual gas remaining within the lung is less than 5 % of VLR. Starting from VLR, the lungs were inflated in 5- or 10-ml steps until the inflation volume approached twice VLR. At this volume the pressure increase for each further step inflation became very large and the slope of the pressure–volume curve decreased dramatically. The system was then deflated in a stepwise fashion until the lungs were completely deflated, and then reinflated to VLR. The steady-state changes in intratracheal pressure associated with this inflation, deflation, reinflation sequence were measured with a Statham P23V pressure transducer and Gould d.c. amplifier and recorded on a Gould series 2600 pen recorder.

Following these measurements, the flank of each turtle, just anterior to the pelvic girdle, was pierced with a 13 gauge hypodermic needle through which a saline-filled cannula (PE 190) was inserted. The needle was then withdrawn and the cannula secured to the flank with a purse-string suture. This cannula was connected to the physiological pressure transducer for the measurement of intra-abdominal pressure during stepwise inflation, deflation and reinflation of the body cavity achieved by inflation and deflation of the lungs, starting from VLR, as described above.

In three animals, following the measurements outlined above, the plastron was removed with a necropsy saw, the pelvic girdle was carefully removed from the shell, and all the viscera including the digestive tract, liver and heart were carefully dissected from the lungs. Once the viscera had been removed, the lungs were inflated to VLR and the steady-state pressures associated with inflation, deflation and reinflation of the isolated lungs were recorded. The exposed lungs were swabbed periodically with saline throughout this procedure to prevent drying.

*Dynamic pressure–volume relationships*

This series of experiments was performed on a further six animals with a mean body weight of 553 ± 81 g, anaesthetized and prepared as described for measurement of the static pressure–volume relationships. In the present series, the tracheal cannula was connected to a Harvard Small Animal Respirator (Harvard Inc., Millis, MA, USA) with a pneumotachograph (Fleish 00) placed in the airflow line leading from the pump to the tracheal cannula. The pressure drop across the pneumotachograph screen during tracheal airflow was measured with a Validyne differential pressure transducer (DP103-18) and this signal was electronically integrated by a Gould integrating amplifier to give the stroke volume of the pump. All measurements of pressure, flow and volume were continuously recorded on the chart recorder and the volume and pressure signals were also plotted simultaneously on an Esterline Angus 575 X-Y plotter. When volume was plotted against pressure on xy coordinates, through a complete pump cycle, a counter-clockwise rotating hysteresis loop was produced (Fig. 3). In three animals, inflation volumes ranging from 1 to 6 ml at pump frequencies ranging from 15 to 60 cycles $min^{-1}$ were used to produce a spectrum of dynamic pressure–volume loops that were within the animals' range of minute ventilation and tidal volume. The selected volumes were absolute values and were kept constant for all animals throughout the experiment. Corrections for the weight of the animal were done during the calculation of mechanical work. All cycles started with the lungs at VLR, and pump volume always started at 6 ml and was sequentially reduced to 1 ml in 1-ml steps at each pump frequency. Frequency was sequentially increased from 15 to 20 cycles $min^{-1}$ and then to 60 cycles $min^{-1}$ in steps of 10 cycles $min^{-1}$. In all six animals, the intra-abdominal pressure and pump stroke volume were also plotted simultaneously, as described above, producing hysteresis loops for the changes in intra-abdominal pressure which accompany changes in the volume of the body cavity during inflation and deflation of the lungs.

*Data analysis*

The static compliances of the total system, body wall and the lungs alone were taken as the slopes of the linear portion of the respective inflation curves, beginning at the origin. Static compliances were standardized to weight and to VLR. The VLR standardized values were used to calculate the percentage of total work required to overcome the elastic forces within the lungs and the body cavity. Pressure–volume loops were analysed to determine the mechanical work required to overcome elastic and non-elastic forces during each pump cycle. Fig. 1 shows a schematic pressure–volume loop with arrows indicating the direction of change in pressure and volume for inspiration (I) and expiration (E). For each pressure–volume loop recorded in the present experiments, a perpendicular line was drawn from the volume axis to the point of peak pressure and volume (line BC in Fig. 1). The area contained within the pressure–volume loop (AICEA = non-elastic work of inflation and deflation) and the area within AICBA (total work of one ventilation cycle) were measured and corrected for weight with an Apple II microcomputer and graphics tablet. During

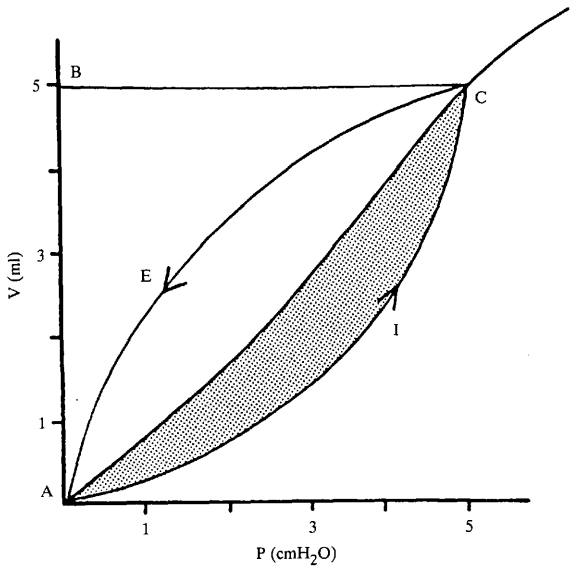


Fig. 1. Schematic diagram of the pressure–volume relationships of the intact respiratory system during a single ventilation cycle. The loop begins at A and is generated by a point moving with time, in a counter-clockwise direction. Shaded area represents the work required to overcome non-elastic forces during inspiration. See text for details. V, inflation volume; P, intrapulmonary or intra-abdominal pressure.

pump ventilation of the anaesthetized animals, expiration was always passive, and non-elastic work for each cycle in these experiments was calculated as half the area of the pressure–volume loop. The work required to overcome the elastic forces in the respiratory system was calculated by subtracting the non-elastic work from the total work in each cycle. These calculations of total, elastic and non-elastic work for each cycle were made on loops obtained for pump ventilation of the intact system and ventilation of the body cavity alone. The work required to ventilate the lungs alone was then calculated by subtracting the work required to ventilate the body cavity from that required to ventilate the total system. Dynamic compliance, the slope of the line connecting the two points of zero flow on the pressure–volume loop, was estimated by calculating the ratio ($\Delta V$) and the corresponding change in pressure ($\Delta P$).

## RESULTS

### *Static pressure–volume relationships*

The static pressure–volume curves for inflation and deflation of the total system, body cavity and lungs of a 639-g turtle are shown in Fig. 2. All curves are generally

sigmoid in shape, indicating that in all cases increasing volume ultimately leads to a disproportionate increase in pressure as the elastic components of the system approach their limits of extensibility. All curves show a pronounced hysteresis between inflation and deflation.

The static compliances derived from the slopes of the mid-range portions of the various inflation curves originating from V and zero pressure are given in Table 1 for all animals examined. The mean compliance of the total system ($C_T$) was 8·4+0·7 ml $cmH_2O^{-1}kg^{-1}$, that of the lungs alone ($C_B$) was 35·1+0·8 ml $cmH_2O^{-1}kg^{-1}$ and that of the body cavity alone ($C_L$) was 11·6+1·4 ml $cmH_2O^{-1}kg^{-1}$. These values are compared to published values for other reptiles and grouped according to lung type as classified by Perry & Duncker (1978) (Table 2).

The percentages of the total work required to overcome elastic forces arising from the body and the lungs on inflation of the intact respiratory system are shown in Table 3. In most reptiles the majority of the elastic recoil resisting inflation arises from the body wall, while the highly compliant lungs offer little resistance to inflation. The one exception is the chameleon, where forces are divided almost equally between the lung and body. In mammals, on the other hand, the majority of

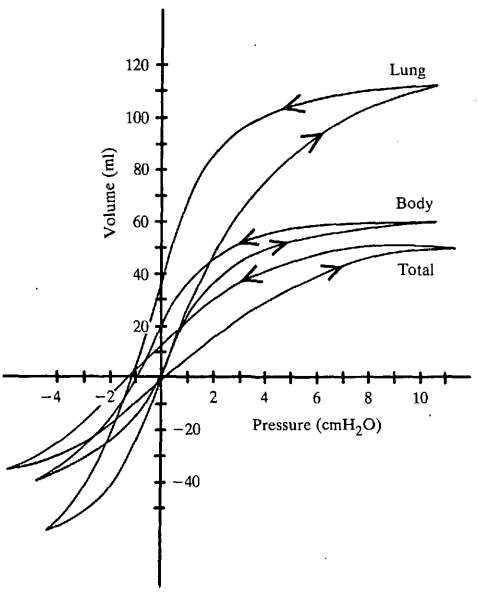


Fig. 2. Pressure–volume curves for the total system (Total), the body wall (Body) and lungs alone (Lung) of a 639-g turtle. Arrows pointing in a positive direction indicate inflation, those pointing in a negative direction indicate deflation.

Table 1. *Values obtained for the compliance of the total system ($C_T$), body wall ($C_B$) and lungs ($C_L$) in ml $cmH_2O^{-1}$ $kg^{-1}$ body weight in* Pseudemys scripta

| | Weight (kg) | $C_T$ | $C_L$ | $C_B$ |
|---|---|---|---|---|
| | 0·733 | 9·2 | 35·8 | 8·4 |
| | 0·437 | 6·8 | 37·0 | 12·1 |
| | 0·639 | 9·1 | 34·2 | 12·4 |
| | 0·750 | | | 9·8 |
| | 0·485 | | | 17·1 |
| | 0·560 | | | 17·3 |
| | 1·467 | | | 10·3 |
| | 0·739 | | | 5·4 |
| $\bar{x}$ | 0·726 | 8·4 | 35·1 | 11·6 |
| ± S.E.M. | 0·107 | 0·65 | 0·78 | 1·35 |

the work done to overcome elastic forces during inflation is required to expand the relatively stiff lungs, while only 25 % of the total elastic work is required to expand the tissues of the body wall.

*Dynamic pressure–volume relationships*

The dynamic pressure–volume relationships of the intact respiratory system of a 750-g animal are shown in Fig. 3 while those obtained for the inflation of the body cavity alone in a 468-g animal are shown in Fig. 4. The curves in Figs 3A and 4A illustrate the effects of increasing stroke volume at a constant ventilation frequency, while Figs 3B and 4B illustrate the effects of increasing ventilation frequency at a constant pump volume. Note that whereas the pressure–volume relationships of the intact system are frequency-dependent, those of the body cavity alone are not. The relationships illustrated in Figs 3 and 4 for the total system and body compartment alone hold true for all pump frequencies at all inflation volumes.

Fig. 5 shows the changes in dynamic compliance of the total respiratory system, as a function of pump frequency, for three pump volumes. Statistically, the dynamic compliance is independent of pump volume over the ranges recorded, although there is a slight trend for the system to behave in a stiffer fashion at higher inflation volumes. The dynamic compliance is, however, strongly frequency-dependent: for any given volume, as frequency increases, the dynamic compliance falls. The decreases in dynamic compliance indicate that the system becomes stiffer with increasing frequency: thus, for any given volume, as frequency increases, the pressure difference generated by inflation also increases. This apparent stiffening of the respiratory system with increasing ventilation frequency is reflected in the work required to produce each breath. Calculated values of the mechanical work required to produce each breath for the total respiratory system, measured from the pressure–volume loops as described above, are shown in Fig. 6. For a constant frequency, increases in $\dot{V}_P$ due to increases in $V_P$ result in a linear rise in W on these log–log curves, indicating an exponential increase in W. If $\dot{V}_P$ is increased by holding volume constant and increasing frequency, W also rises but in a non-linear fashion. Thus the

Table 2. *Values recorded for the compliance of the total system ($C_T$), body wall ($C_B$), and lungs ($C_L$) for various species standardized to body weight and to resting lung volume ($V_{LR}$)*

| Animal | Lung type | $C_T$ (ml $cmH_2O^{-1}$ $kg^{-1}$) | $C_L$ (ml $cmH_2O^{-1}$ $kg^{-1}$) | $C_B$ (ml $cmH_2O^{-1}$ $kg^{-1}$) | $C_T$ (ml $cmH_2O^{-1}$ $ml^{-1}$ $V_{LR}$) | $C_L$ (ml $cmH_2O^{-1}$ $ml^{-1}$ $V_{LR}$) | $C_B$ (ml $cmH_2O^{-1}$ $ml^{-1}$ $V_{LR}$) | Source |
|---|---|---|---|---|---|---|---|---|
| Green lizard (*Lacerta viridis*) | unicameral | 18·20 | 62·10 | 26·70* | 0·53 | 1·78 | 0·76* | Perry & Duncker (1978) |
| Tokay gekko (*Gekko gecko*) | unicameral | 47·10 | 273·40 | 56·9* | 0·73 | 4·07 | 0·89* | Perry & Duncker (1978) |
| Tokay gekko (*Gekko gecko*) | unicameral | 16·0 | 201·6 | 14·5 | 0·25 | 3·17 | 0·23 | Milsom & Vitalis (1984) |
| Chameleon (*Chameleo chameleon*) | paucicameral | 305·70 | 759·00 | 511·8* | 2·50 | 5·73 | 3·84* | Perry & Duncker (1978) |
| Monitor lizard (*Varanus exanthematicus*) | multicameral | 66·80 | 365·50 | 82·20* | 0·66 | 3·27 | 0·83* | Perry & Duncker (1978) |
| Red eared turtle (*Pseudemys scripta*) | multicameral | 10·00 | 170·00 | 10·60* | 0·10 | 1·70 | 0·11* | Jackson (1971) |
| Red eared turtle (*Pseudemys scripta*) | multicameral | 8·40 | 35·10 | 11·60 | 0·08 | 0·35 | 0·12 | Present study |
| Rat (*Ratus* sp.) | broncho-alveolar | 0·91 | 1·56 | 2·20 | 0·09 | 0·12 | 0·55 | Crosfill & Widdicombe (1961) |

* Values for $C_B$ calculated from the formula $1/C_B = 1/C_T - 1/C_L$. Other values for $C_B$ were derived experimentally.

Table 3. *Percentage of the total work required to overcome the elastic forces resisting static lung inflation which arise from the body wall and lung*

| Animal | Lung (%) | Body (%) | Source |
|---|---|---|---|
| Green lizard | 30 | 70 | Perry & Duncker (1978) |
| Tokay gekko | 18 | 82 | Perry & Duncker (1978) |
| Tokay gekko | 8 | 92 | Milsom & Vitalis (1984) |
| Chameleon | 44 | 56 | Perry & Duncker (1978) |
| Monitor lizard | 20 | 80 | Perry & Duncker (1978) |
| Red eared turtle | 8 | 92 | Jackson (1971) |
| Red eared turtle | 23 | 77 | Present study |
| Mammal (rat) | 75 | 25 | Crosfill & Widdicombe (1961) |

Calculations were based on compliance values standardized to VLR.

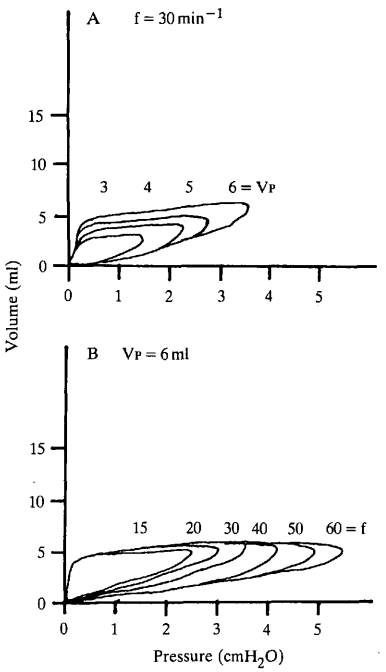


Fig. 3. Effects of changes in ventilation frequency (f) and volume (VP) on the pressure–volume (P–V) loops of the intact respiratory system associated with single pump ventilation cycles in a 750-g turtle. (A) The effect of increasing pump volume from 3 to 6 ml on pressure–volume loops at a constant ventilation frequency of 30 cycles $min^{-1}$. (B) The effect of increasing ventilation frequency on pressure–volume loops for a constant pump volume of 6 ml.

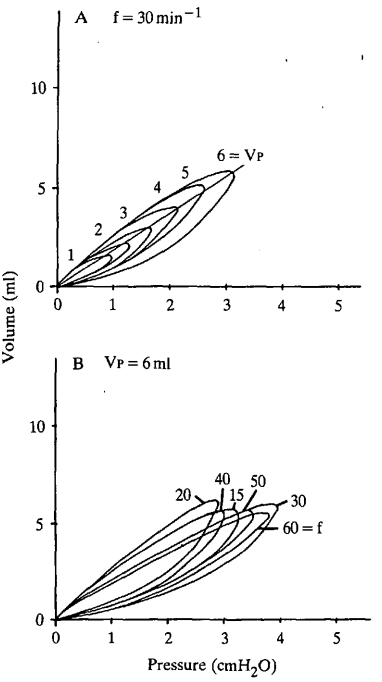


Fig. 4. Effects of changes in ventilation frequency (f) and volume ($V_P$) on the pressure–volume (P–V) loops of the body compartment alone associated with single pump ventilation cycles in a 468-g animal. (A) The effect of increasing pump volume from 1 to 6 ml on pressure–volume loops at a constant ventilation frequency of 30 cycles min$^{-1}$. (B) The effect of increasing ventilation frequency for a constant pump volume of 6 ml.

rise in W, with increasing levels of f at constant $V_P$, is small at $f < 30$ cycles min$^{-1}$, and rises sharply with $f > 30$ cycles min$^{-1}$. The total work required to produce each breath can be subdivided into the work required to overcome elastic and non-elastic forces (Otis *et al.* 1950). Fig. 7 shows that, whereas the work required to overcome both elastic and non-elastic forces is roughly equal at low pump volumes and frequencies, the work required to overcome non-elastic forces becomes the major component of the total work at larger stroke volumes and higher pump frequencies.

The work required to produce a single breath can also be analysed in terms of the work required to inflate the lung and the work required to inflate the body compartment, since the pressure within the respiratory system is the sum of the pressures contributed by the lung and body wall (Agostoni, 1970). Fig. 8 shows the contribution of the lung and body wall to the total work required to produce a single breath at pump volumes of 2 and 6 ml with increasing pump frequencies. The work

required to overcome the forces within the body wall are volume-dependent and increase with stroke volume. This component of the total work, however, is relatively frequency-independent. As a consequence, rises in the total work required to produce each breath as $\dot{V}_P$ increases are a result of frequency-dependent increases in the work required to inflate the lungs.

The values of the work required to produce each breath from Fig. 6 are replotted in Fig. 9 as minute work ($\dot{W}$), the product of the work required to produce each breath and the number of breaths produced each minute (f). For any given level of minute pump ventilation, $\dot{W}$ initially falls as f increases and $\dot{V}_P$ decreases until $\dot{W}$ reaches a minimum. Further increases in f and decreases in $\dot{V}_P$ produce a rise in $\dot{W}$. The absolute levels of $\dot{W}$ increase and the shape of this curve becomes accentuated at higher levels of $\dot{V}_P$.

For $\dot{V}_P$ values ranging from 100 to 300 ml $min^{-1}$, $\dot{W}$ is minimum at frequencies between 35 and 45 cycles $min^{-1}$. Minute work is analysed in terms of the work required to overcome elastic and non-elastic forces for a $\dot{V}_P$ of 200 ml $min^{-1}$ in

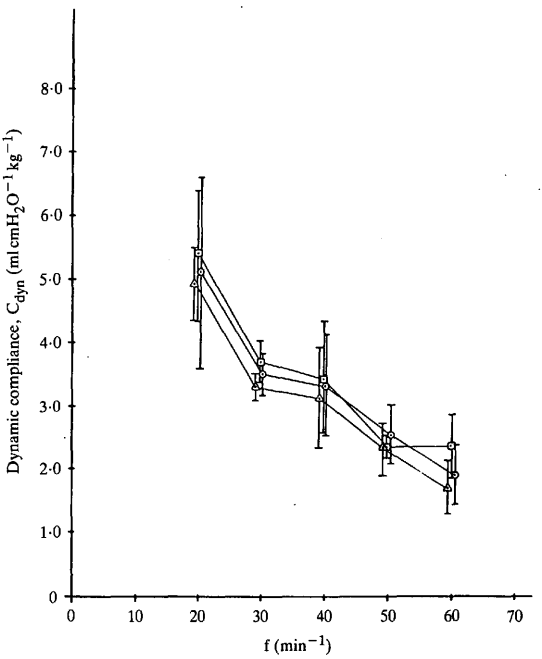


Fig. 5. The relationship between ventilation frequency (f) and dynamic compliance ($C_{dyn}$) for constant pump volumes of 2 (□), 4 (○) and 6 (△) ml. Each point represents the mean value for three animals. Vertical bars indicate the S.E.M.

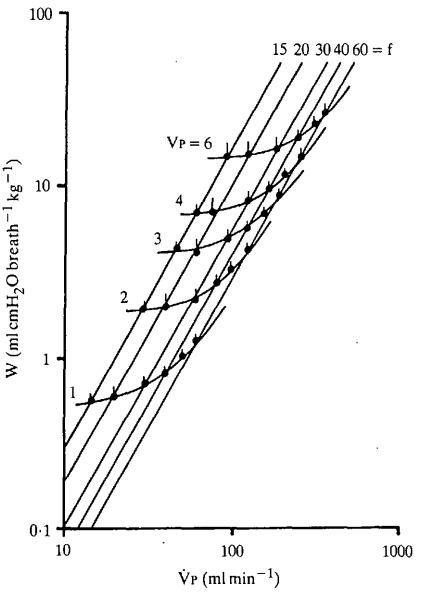


Fig. 6. The relationship between the total work per breath (W) and minute pump ventilation ($\dot{V}_P$) for different combinations of pump volume ($V_P$ in ml) and pump frequency (f in cycles $min^{-1}$). Data represent average values from three animals. Vertical bars indicate S.E.M.

Fig. 10B. As pump frequency increases, the minute work done to overcome elastic forces drops sharply and then stabilizes or rises very slightly as f continues to increase. The work required to overcome non-elastic forces increases slowly over the entire frequency range. The minute work required to overcome both elastic and non-elastic forces sum to give a resultant 'U' shape to the total minute work curve. This effect becomes more pronounced as $\dot{V}_P$ increases.

In Fig. 10A total minute work is broken down into the components required to ventilate the lungs and the body cavity. The minute work required to overcome the forces within the body cavity for a $\dot{V}_P$ of 200 ml $min^{-1}$ steadily declines as f increases. The minute work required to overcome the forces within the lungs as pump frequency increases, however, declines initially and then rises, causing the total minute work curve to be 'U' shaped. Again these effects are more pronounced at higher levels of $\dot{V}_P$.

## DISCUSSION

The compliance of the total respiratory system of the turtle, *Pseudemys scripta*, measured in this study, is in general agreement with results obtained for the

same species by Jackson (1971). He reported values for lung compliances (170 ml $cmH_2O^{-1}kg^{-1}$), however, which were much higher than those measured in the present study (35·1 ml $cmH_2O^{-1}kg^{-1}$). This is probably because he used different methods. In Jackson's (1971) study, the compliance of the exposed lung was determined beginning at atmospheric pressure with the lungs completely collapsed. In the present study the static inflation curve was determined beginning with the exposed lungs inflated to VLR. As a consequence, CL was determined at a greater lung volume which may have corresponded to a stiffer portion of the pressure–volume curve.

Since the lungs and body are placed in series, the algebraic sum of the pressure exerted by these two component parts must equal the pressure exerted by the total respiratory system (Agostoni, 1970). Since compliance is equal to $\Delta V/\Delta P$, it follows that for any given value of V, the sum of the reciprocals of the lung compliance and the body compliance must equal the reciprocal of the compliance of the total system:

$$\frac{1}{C_L} + \frac{1}{C_B} = \frac{1}{C_T}.$$

If the values of CT and CB measured in the present study are substituted into this equation, CT is calculated as 30·5 ml $cmH_2O^{-1}kg^{-1}$, which is close to the

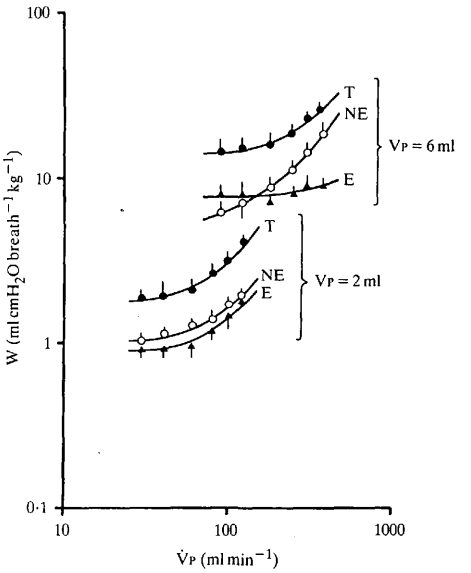


Fig. 7. The contribution of elastic (E) and non-elastic (NE) work per breath (T) for VP of 2 ml and 6 ml with changing levels of minute pump ventilation ($\dot{V}P$). Each point represents the mean value of three animals. Vertical bars indicate S.E.M.

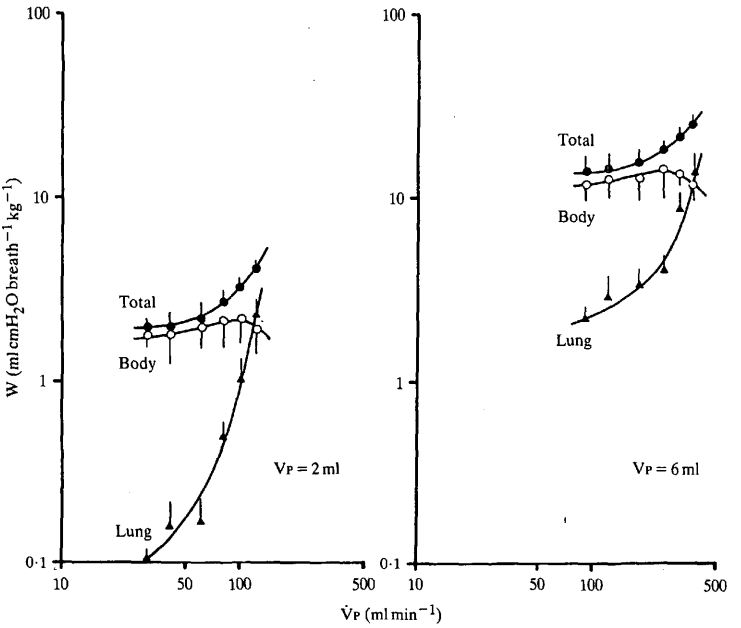


Fig. 8. The relative proportion of the work required to inflate the lungs ($N = 3$) and body ($N = 6$) compared to the total ($N = 3$) work per breath (W) for pump volumes ($V_P$) of 2 ml and 6 ml with changing levels of minute pump ventilation ($\dot{V}_P$). Vertical bars indicate S.E.M.

experimentally derived value of $35{\cdot}1\,\text{ml}\,\text{cmH}_2\text{O}^{-1}\,\text{kg}^{-1} \pm 0{\cdot}78$ (S.E.M.) for lung compliance. Thus the compliance of the lung as measured in this study is consistent with the experimentally derived values for body compliance and total respiratory system compliance.

The results of the present study further indicate that the compliance of the total respiratory system of this species of turtle is determined mainly by the compliance of the body wall. Only 23 % of the forces resisting inflation within this system arise from the lungs. Using the values for $C_T$ and $C_L$ reported by Jackson (1971), the elastic contribution is calculated at only 8 % of the total elastic forces resisting inflation. The percentage of elastic resistance to inflation offered by the lungs, as calculated in this study, lies well within the range of values calculated for other reptiles (8–44 %), whereas the value calculated from Jackson (1971) lies at the lower extreme.

A comparison of compliance values for the total respiratory system, body wall and lungs of various species of reptiles indicates that the respiratory system of turtles is relatively stiff (Table 3). The lizards, for instance, have a system that is 2 to 30 times more compliant than the chelonian respiratory system. The relatively stiff

respiratory system of the turtle can be attributed to the animal's shell. The ribs of the turtle are fused to the dome of the carapace and are immobile. The only portions of the animal's body capable of distension upon inflation are the flank cavities and the pectoral girdle. The lizards, on the other hand, have articulated ribs capable of moving as the lungs inflate and the volume of the body cavity increases. The multicameral lungs of the turtle, with their internal septation, are somewhat stiffer than the unicameral or paucicameral lungs of lizards (Table 3). Interspecific comparisons of compliance values normalized to body weight show that the compliance of the respiratory system of lizards is much greater than that of chelonians and that chelonians possess a more compliant system than mammals ($C_T$ for lizards is 2–30 times greater than $C_T$ for turtles which is 9–10 times greater than $C_T$ for rats). Comparisons made on a volume basis (normalized to resting lung volume) again show that lizards have the highest compliance values, but the chelonian and mammalian systems have similar values ($C_T$ for lizards is 5–23 times $C_T$ for turtles which is approximately equal to $C_T$ for rats). In mammals, however, $C_T$ is determined primarily by the lungs, which contribute 75 % of the elastic forces resisting inflation in the respiratory system. Turtles, on the other hand, have relatively compliant lungs compared to those of mammals and $C_T$ is predominantly determined by the body

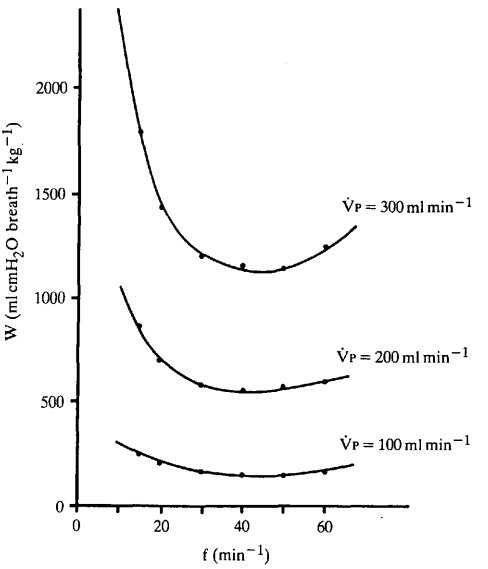


Fig. 9. The relationship between the rate of work ($\dot{W}$) and ventilation frequency (f in cycles $min^{-1}$) for various constant levels of minute pump ventilation ($\dot{V}_P$ in ml $min^{-1}$). These curves were derived from the points presented in Fig. 6.

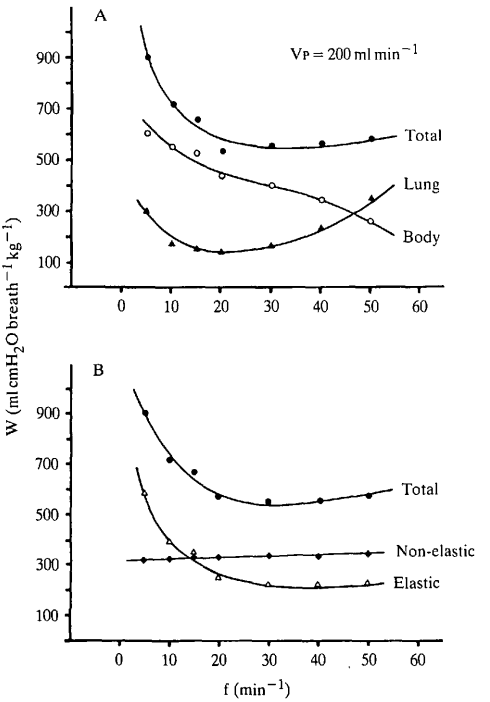


Fig. 10. (A) The minute work ($\dot{W}$) required to ventilate the lungs, the body compartment and the total system at the same constant level of minute ventilation with increasing pump frequency. These curves were derived from data presented in Figs 6 and 8. (B) The amount of total minute work ($\dot{W}$) required to overcome elastic and non-elastic forces at a constant minute pump ventilation ($\dot{V}_P$) of 200 ml min$^{-1}$ with increasing pump frequency (f in cycles min$^{-1}$). These curves were derived from data presented in Figs 6 and 7.

wall, which contributes 77% of the elastic forces within the respiratory system resisting inflation.

Perry & Duncker (1978) claim that high lung compliance in reptiles is associated with the degree of development of caudal and ventral dilations in the lung: the development of these membraneous regions is most extensive in the chameleon, followed by the Tokay gekko and savanna monitor (Table 3). The data of the present study, however, do not support this trend in the relationship between lung volume, general internal architecture of the lung and lung compliance. Whether the comparisons are made using values standardized to body weight or to resting lung volume, $C_T$ is much lower than would be predicted given the lung volume and lung architecture of this species. It may be the case that this trend is only found in the

lizards or is merely a consequence of the small sample size used by Perry & Duncker (1978).

Under dynamic conditions, the compliance of the respiratory system shows frequency dependence, but little or no dependence on $V_P$ over the range studied. The frequency dependence of the dynamic compliance ($C_{dyn}$) must arise from a change in stiffness of the lungs with changing frequency, as there is no frequency dependence in $C_{dyn}$ for the body cavity alone (Fig. 6). In the Tokay gekko, the respiratory system showed a frequency-dependent decrease in $C_{dyn}$ which was enhanced by increasing ventilation volume at high ventilation frequencies (Milsom & Vitalis, 1984). This dependence of $C_{dyn}$ on pump volume at high ventilation frequencies in the Tokay gekko was thought to be the result of the visco-elastic properties of the body wall. The absence of such an effect in the present study may be because the turtle has a shell and therefore does not experience geometric change with increasing volume, leaving the membranes of the flank cavities and the pectoral girdle as the sole visco-elastic elements. It is more probable, however, that the volume effects on the frequency dependence of $C_{dyn}$ only appear at larger pump volumes. The pump volumes used in the present study were only 2–6 % of resting lung volume, whereas in the study on the Tokay gekko the pump volumes used were 10–50 % of resting lung volume. The dependence of $C_{dyn}$ on frequency observed in the turtle means that a greater change in pressure will result for any given change in volume as frequency increases. This is reflected in the measurements of the total work breath$^{-1}$ obtained for the total respiratory system.

For any given pump volume, the work required to produce a single breath increases as frequency increases, with the slope of the rise in W being small at low frequencies but increasing sharply above 30 cycles min$^{-1}$. This is primarily due to an increase in the work required to overcome non-elastic forces within the lung. The work required to inflate the body wall and body cavity is relatively frequency-independent and primarily required to overcome elastic forces. Thus, although at low pump frequencies the majority of work must be done to overcome elastic forces in the body wall, at higher frequencies the majority of the work is required to overcome non-elastic forces in the lungs.

For any given ventilation frequency, the work required to produce each breath increases exponentially as pump volume increases. The work required to overcome elastic forces in the body wall, body cavity and lungs accounts for approximately 50 % of the total work at low pump volumes, but the work required to overcome non-elastic forces contributes the major portion to the total work of ventilation at high pump volumes because of the necessary increases in flow rates and thus flow resistance and viscous effects. The intrapulmonary bronchi and the trachea are the most probable sites for flow resistance in the respiratory system of turtles, and, even though turtles do not possess a highly branched bronchial tree as in mammals, it is not surprising that flow resistance is found in their lungs. Because of the large cross sectional area of the lower portion of the bronchial tree in mammals, little flow resistance occurs below the medium-sized bronchi, with the majority of flow resistance being in the upper airways (Pedley, Schroter & Sudlow, 1970). The

minute work ($\dot{W}$) required to maintain a constant level of minute ventilation ($\dot{V}_P$) is a product of the work required to produce each breath multiplied by the pump frequency. When $\dot{W}$ is expressed as a function of f for constant levels of $\dot{V}_P$, the resulting curves demonstrate that there is a combination of f and $V_P$ at which the work of ventilation is minimal. At pump frequencies below this level, minute work increases as $V_P$ increases, primarily due to an increase in the work required to overcome elastic forces in the body wall. At pump frequencies above this level, minute work increases primarily as a result of an increase in the work required to overcome non-elastic (flow-resistive) forces in the lung.

The work required to inflate the lungs as a percentage of the total work of breathing increases in the sequence gecko > turtle > mammal. This hierarchy also reflects the increasing complexity of lung architecture. Given the simple structure of their lungs, the total work of breathing in the Tokay gecko is almost entirely required to overcome elastic forces arising from the body wall at all frequencies and tidal volumes (Milsom & Vitalis, 1984). In turtles, the mechanical work required to inflate the respiratory system is divided equally between overcoming elastic and non-elastic forces at low pump frequencies and volumes with almost all of these forces residing in the body wall and cavity. The work required to overcome non-elastic forces, however, predominates at high frequencies and tidal volumes, with the lungs contributing an increasing portion of this work. In mammals, the work required to inflate the respiratory system is primarily required to overcome elastic forces at low pump frequencies and non-elastic forces at high pump frequencies, but in both instances these forces reside primarily in the lungs (Otis *et al.* 1950). The present results and the above comparisons would suggest that, whereas differences in the structure and rigidity of parts of the body wall can have significant effects on pulmonary mechanics, far more profound effects arise in conjunction with differences in lung architecture. Although these differences were not evident from the static compliance curves, which only provide information on elastic forces, the dynamic measurements show that lungs of increasing complexity become progressively more important in determining the overall mechanics of the respiratory system. The role of mechanical factors in determining breathing patterns in turtles is complex. From the mechanical analysis one would predict that the most energetically favourable breathing pattern is one that occurs at 40 breaths $min^{-1}$. This prediction is based on the power curves for continuous ventilation presented in Fig. 9. Turtles, however, breath intermittently not continuously and therefore have a very low breathing frequency. The interpretation of intermittent breathing in the light of the present mechanical analysis is considered in the following study (Vitalis & Milsom, 1986).

## REFERENCES

AGOSTONI, E. (1970). Statics. In *The Respiratory Muscles* (ed. G. M. J. Cambell, E. Agostoni & J. Newsome Davis). London: Lloyd-Luke Ltd.

AGOSTONI, E. B., THIMM, F. F. & FENN, W. O. (1959). Comparative features of the mechanics of breathing. *J. appl. Physiol.* **14**, 679–683.

BENCHETRIT, B. & DEJOURS, P. (1980). Ventilatory $CO_2$ drive in the tortoise *Testudo horsfieldi*. *J. exp. Biol.* **87**, 229–236.

CHRISTIE, R. V. (1953). Dyspoena in relation to the visco-elastic properties of the lungs. *Proc. R. Soc. exp. Biol. Med.* **46**, 381–386.

CRAGG, P. A. (1978). Ventilatory patterns and variables in rest and activity in the lizard, *Lacerta*. *Comp. Biochem. Physiol.* **60**A, 399–410.

CROSFILL, M. L. & WIDDICOMBE, J. G. (1961). Physical characteristics of the chest and lungs and the work of breathing in different mammalian species. *J. Physiol., Lond.* **158**, 1–14.

GANS, C. & CLARK, B. (1976). Studies on ventilation of *Caimen crocodilus* (Crocodilia: Reptilia). *Respir. Physiol.* **26**, 285–301.

GANS, C. & HUGHES, G. M. (1967). The mechanism of lung ventilation in the tortoise, *Testudo graeca* Linne. *J. exp. Biol.* **47**, 1–20.

GLASS, M. L. & JOHANSEN, K. (1976). Control of breathing in *Acrochordus javanicus*, an aquatic snake. *Physiol. Zöol.* **49**, 328–340.

GLASS, M. L. & WOOD, S. C. (1983). Gas exchange and control of breathing in reptiles. *Physiol. Rev.* **63**, 232–260.

JACKSON, D. C. (1971). Mechanical basis for lung volume variability in the turtle *Pseudemys scripta elegans*. *Am. J. Physiol.* **220**, 754–758.

MCCUTCHEON, F. H. (1943). The respiratory mechanism in turtles. *Physiol. Zool.* **16**, 255–269.

MILSOM, W. K. & JONES, D. R. (1980). The role of vagal afferent information and hypercapnia in control of the breathing pattern in Chelonia. *J. exp. Biol.* **87**, 53–63.

MILSOM, W. K. & VITALIS, T. Z. (1984). Pulmonary mechanics and the work of breathing in the lizard, *Gekko gecko*. *J. exp. Biol.* **113**, 187–202.

NAIFEH, K. H., HUGGINS, S. E., HOFF, H. E., HUGG, T. W. & NORTON, R. E. (1970). Respiratory patterns in crocodilian reptiles. *Respir. Physiol.* **9**, 31–42.

OTIS, A. B., FENN, W. O. & RAHN, H. (1950). Mechanics of breathing in man. *J. appl. Physiol.* **2**, 592–603.

PEDLEY, T. J., SCHROTER, R. C. & SUDLOW, M. F. (1970). The prediction of pressure drop and variation of resistance within the human bronchial airways. *Respir. Physiol.* **9**, 387–405.

PERRY, S. F. & DUNCKER, H. R. (1978). Lung architecture, volume and static mechanics in five species of lizards. *Respir. Physiol.* **34**, 61–81.

PERRY, S. F. & DUNCKER, H. R. (1980). Interrelationship of static mechanical factors and anatomical structure in lung evolution. *J. comp. Physiol.* **138**, 321–334.

WOOD, S. C. & LENFANT, C. J. M. (1976). Respiration: Mechanics, control and gas exchange. In *Biology of the Reptilia* (ed. C. Gans & W. R. Dawson). New York: Academic Press.

YAMASHIRO, S. M., DAUBENSPECK, J. A., LAURITSEN, T. N. & GRODINS, F. S. (1975). Total work rate of breathing optimization in $CO_2$ inhalation and exercise. *J. appl. Physiol.* **38**, 702–709.

VITALIS, T. Z. & MILSOM, W. K. (1986). Mechanical analysis of spontaneous breathing in the semi-aquatic turtle, *Pseudemys scripta*. *J. exp. Biol.* **125**, 157–171.